

# Interrelation between Primary and Secondary Relaxations in Polymerizing Systems Based on Epoxy Resins

M. Beiner\*

Fachbereich Physik, Universität Halle, D-06099 Halle (Saale), Germany

K. L. Ngai

Naval Research Laboratory, Washington, D.C. 20375-5320

Received February 22, 2005; Revised Manuscript Received June 13, 2005

**ABSTRACT:** There is a wealth of experimental data published on the change of molecular dynamics of epoxy resins during polymerization reaction. Common aspects are an increase of the primary  $\alpha$ -relaxation time  $\tau_\alpha$  and a broadening of the  $\alpha$ -relaxation process during the polymerization reaction. In this paper we discuss systematic changes in the two secondary relaxations  $\beta$  and  $\gamma$  on the way from a neat molecular glass-former to the fully polymerized state based on literature data and new dielectric results for diglycidyl ether of bisphenol A (DGEBA) cured with ethylenediamine (EDA). The discussion is focused on common trends in the relaxation time  $\tau_\beta$  which were not reported previously. It is shown that the relative changes of  $\tau_\alpha$  and  $\tau_\beta$  during the polymerization process are in accord with the predictions of the coupling model and that it is the  $\beta$ -relaxation which is the initiator of the  $\alpha$ -relaxation of the epoxy resins in its neat state as well as the initiator of the local segmental relaxation of polymerized or cross-linked epoxy resins. In the terminology of small molecular glass-forming substances, the  $\beta$ -relaxation of the epoxy resins would be called the Johari–Goldstein process.

## 1. Introduction

Over the past two decades, a large number of papers<sup>1–15</sup> have been published to study the evolution of the primary and secondary relaxations in the glassy and supercooled liquid states of various epoxy resins and epoxy-based mixtures forming polymer networks or linear chains by condensation reaction. An objective of many works is to obtain physical insight into the slowing of the molecular dynamics when a macromolecule grows from a simple molecular substance. Various experimental techniques have been used, including dielectric relaxation spectroscopy,<sup>2–4</sup> shear measurements,<sup>5,6</sup> microwave absorption, ultrasound,<sup>7</sup> and calorimetry.<sup>8</sup> Studies by Johari and co-workers<sup>2,9–13</sup> and other groups<sup>3,4,14,15</sup> provide detailed information on the dielectric relaxation behavior, which is the subject of this work. Well investigated are cross-linking and polymerization processes of diglycidyl ether of bisphenol A (DGEBA) supplied by Shell Chemicals under the trade name EPON828. Its number-average molecular weight is 380 Da. Its glass transition temperature is 255 K, and its functionality (the number of reacting terminal epoxy groups per molecule) is 2.0. When EPON828 is mixed with a polymerizing or cross-linking agent, being a second molecular substance, in some proportion to ensure stoichiometry polymerization or network formation occurs. From stoichiometric mixtures of 1 mol of monoamines like aniline or cyclohexylamine (CHA) with 1 mol of the diepoxide EPON828, one gets as an ultimate product after completion of reaction a linear chain macromolecule. EPON828 cured with cross-linking agents like *p*-aminodicyclohexylmethane (PACM) or ethylenediamine (EDA) gives ultimately a polymer network.<sup>13</sup> Stoichiometry of the polymerization reaction requires in this case 1 mol of PACM or EDA to be mixed with 2 mol of EPON828. Instead of the diepoxide

EPON828, a triepoxide, triphenylolmethane triglycidyl ether (TPMTGE) with the trade name Tactix742 and average molecular weight of 480 Da, has been used in other studies.<sup>10</sup>

In the past, dielectric spectra of epoxy systems have been measured at various stages of the polymerization process, and the properties of the secondary and primary relaxations as well as their changes from stage to stage are known. In time order, the stages are (1) the neat EPON828<sup>16</sup> or neat Tactix742,<sup>17</sup> (2) the unreacted mixtures of EPON828 with aniline, CHA,<sup>9,10,12</sup> or PACM<sup>13</sup> or unreacted mixtures of Tactix742 with the monoamines 3-chloroaniline or 4-chloroaniline,<sup>10</sup> (3) the partially polymerized products at different instants of reaction, and (4) the completely polymerized product. The observed molecular dynamics at each stage as well as the changes from one stage to another present multiple challenges for interpretation and explanation.

In this work we add new experimental data for mixtures of EPON828 with ethylenediamine (EDA), which form a covalently bonded polymer network. Stoichiometric mixtures containing 2 mol of EPON828 and 1 mol of EDA with purity of about 99.5% (Aldrich) are studied. Dielectric measurements have been performed to obtain the spectra in real time during the polymerization process as well as information about secondary relaxations in polymer networks formed after isothermal polymerization at different temperatures. Dielectric sweeps in the frequency range 100 Hz–10 MHz are measured during the cross-linking process using a HP 4192A LCR bridge. Temperature-dependent measurements on isothermally cross-linked samples are performed in the frequency range 0.1 Hz–1 MHz with a Novocontrol instrument based on a Schlumberger 1240 analyzer. Isothermal data in the high-frequency range 100 MHz–1 GHz are measured at room temperature using a HP 4291A RF analyzer in combination with a homemade sample cell. This experimental work

\* Corresponding author. E-mail: beiner@physik.uni-halle.de.

covers stages 3 and 4 of the polymerization process discussed above.

The effects observed in the different stages do not depend basically upon the nature of the polymeric structure formed, chemical or architectural, but mainly on the dynamical constraints to dipolar reorientation. We expect that an understanding of the changes in the dynamics during the formation of macromolecules from much simpler molecules would be an important step to understand general aspects of the dynamics in glass-forming materials. The foundation of interpreting the changes in terms of a structural feature, namely, the number of covalent bonds formed,  $N(t)$ , have been already laid in previous works.<sup>2,9–13</sup> Thus, we use this terminology below to characterize the stage of the polymerization process although experimental  $N(t)$  values are not always available. Increase of  $N(t)$  leads to increasing configurational restrictions on molecular diffusion and decreasing configurational entropy. The specific volume was observed to decrease in the experiments. On the basis of the coupling model (CM),<sup>18–22</sup> further interpretations can be made considering the molecular dynamics at each stage and the relation between stages. Some experimental facts that have not been exploited previously are brought out in this way. The CM addresses the slowing of the primary  $\alpha$ -relaxation by many-body dynamics caused by intermolecular interactions or configurational constraints. This is conceptually related to the interpretation by Johari et al. that configurational restrictions increase and configurational contributions to the volume, enthalpy, and entropy decrease when the number of covalent bonds is irreversibly increased by condensation reactions at a fixed temperature. Thus, it seems natural to use the CM for further interpretations. Moreover, it was discussed recently that the CM makes a distinction of one kind of secondary relaxation (the Johari–Goldstein relaxation)<sup>23,24</sup> which is instrumental in the many-body dynamics and giving rise to the primary relaxation. A fundamental relation exist between the relaxation time of this kind of secondary relaxation and that of the primary relaxation.<sup>18–22,24–26</sup> On the other hand, such relation does not exist for secondary relaxations which are not of the Johari–Goldstein kind. Both kinds of secondary relaxation seem to be present in the diepoxide and the triepoxide, their mixtures with amines, and partially polymerized products. The properties of these two kinds of secondary relaxations and their relations to the primary relaxation change with the stage of the polymerization process. The observed changes are compared with the predictions of the coupling model in this paper.

## 2. Relation between $\alpha$ -Relaxation and JG $\beta$ -Relaxation from the Coupling Model

The coupling model (CM)<sup>18–22</sup> emphasizes the many-molecule nature of the  $\alpha$ -relaxation dynamics of a glass-former through the intermolecular coupling of the relaxing species with others in its environment. Rigorous solution of the simple coupled system<sup>17</sup> has given support to the premise of the CM. First we restate in brief the physical basis of the CM before extending it to include the JG relaxation. The many-molecule  $\alpha$ -relaxation is dynamically heterogeneous and evolves with time, and the details are extremely difficult to describe. At this time, a complete and rigorous solution of this problem has not been given. Although this lofty goal

cannot be realized for some time to come, progress can be made by a simplified model that captures some of the essential physics and has predictions that can be verified or falsified by experiments. An example of this simplified model is the CM which recognizes that the many-molecule dynamics, despite its complexity, originate from independent or primitive motion of individual molecules. Attempts of relaxation of individual molecules have the primitive rate  $\tau_0^{-1}$ , but the many-molecule dynamics prevents all attempts of molecules to be simultaneously successful, resulting in faster and slower relaxing molecules or heterogeneous dynamics. However, when averaged over all molecules, the effect is equivalent to the slowing down of  $\tau_0^{-1}$  by another multiplicative factor, which is time dependent. The time-dependent rate  $W(t)$  has the product form  $\tau_0^{-1}f(t)$ , where  $f(t) < 1$ . In particular, it is

$$W(t) = \tau_0^{-1}(\omega_c t)^{-n} \quad (1)$$

with  $\omega_c$  being the frequency, where the crossover from simple to fractional exponential relaxation occurs, and  $0 \leq n < 1$ , in order that the solution of the averaged rate equation is the empirical Kohlrausch–Williams–Watts (KWW) stretched exponential function for neat glass-formers

$$\phi(t) = \exp[-(t/\tau_\alpha)^{1-n}] \quad (2)$$

Here  $n$  is the coupling parameter of the CM and  $\beta \equiv (1 - n)$  is the fractional KWW exponent. In the case of pronounced many-molecule dynamics (or dynamic heterogeneity) we expect larger coupling parameters  $n$  and vice versa. The time-dependent rate  $\tau_0^{-1}(\omega_c t)^{-n}$  also leads immediately to the most important relation between  $\tau_\alpha$  and  $\tau_0$  of the CM given by

$$\tau_\alpha = (t_c^{-n} \tau_0)^{1/(1-n)} \quad (3)$$

after identifying  $t_c$  introduced here by  $t_c = (1 - n)^{-(1/n)}/\omega_c$ . Many-molecule dynamics do not start instantly. In fact, experiments and molecular dynamics simulations of polymeric and small molecular liquids performed at short times show<sup>18c</sup> that the KWW function no longer holds at times shorter than  $\sim 2$  ps and is replaced by the linear exponential time dependence of the primitive relaxation. The transport coefficients, including viscosity and conductivity, assume the Arrhenius temperature dependence of the primitive relaxation when the relaxation time becomes less than 2 ps.<sup>27</sup> These properties indicate that  $t_c$  is equal to 2 ps for molecular and polymeric glass-formers. The magnitude of  $t_c$  is determined by the intermolecular potential; a weaker potential leads to a longer  $t_c$ . The Lennard-Jones potential,  $V(r) = 4\epsilon[(\sigma/r)^{12} - (\sigma/r)^6]$ , is often used to model the intermolecular potential of molecular and polymeric glass-formers in molecular dynamic simulations. The unit of time from the Lennard-Jones potential is given by  $(m\sigma^2/48\epsilon)^{1/2}$ , and typically its order of magnitude is 1 ps from the parameters chosen for molecular and polymeric glass-formers. It is gratifying to see the experimentally determined value of  $t_c$  is comparable in order of magnitude to the Lennard-Jones unit of time.

Recently, the CM described above has been extended to make the connection of its primitive relaxation time  $\tau_0$  with the most probable relaxation time of the Johari–

Goldstein (JG) secondary relaxation  $\tau_\beta$ .<sup>19–22,24–26</sup> Such a connection is expected from the similar characteristics of the two relaxation processes, including their local nature, involvement of essentially the entire molecule, and both acting as the precursor of the  $\alpha$ -relaxation. Multidimensional NMR experiments<sup>28</sup> have shown that in the systems studied molecular reorientation in the heterogeneous  $\alpha$ -relaxation (executed by the primitive relaxation in the framework of the CM) occurs by relatively small jump angles, just like in the JG relaxation.<sup>29</sup> Since it may seem to the reader that there is now yet another role played by the primitive relaxation, *separate and distinctive* from that described in the above for the Kohlrausch  $\alpha$ -relaxation, it is necessary to give the following clarifications. At short times, when there are few independent relaxations present, they appear separately in space as localized motions just like the JG relaxation. Hence

$$\tau_\beta(T,P) \approx \tau_0(T,P) \quad (4)$$

and this is one role played by the independent relaxation. On combining eqs 3 and 4, we obtain a relation between  $\tau_\alpha$  and  $\tau_\beta$  given by

$$\tau_\alpha(T,P) = [t_c^{-n} \tau_\beta(T,P)]^{1/(1-n)} \quad (5)$$

which should be valid for each equilibrium state characterized by temperature  $T$  and pressure  $P$ . At times beyond  $\tau_0$  or  $\tau_\beta$ , more units can independently relax. However, they cannot be considered as isolated events anymore, and some degree of cooperativity (or dynamic heterogeneity) is required for motions to be possible. The degree of cooperativity and the corresponding length scale continue to increase with time as more and more units participate in the motion, as suggested by the evolution of dynamics of colloidal particles with time obtained by confocal microscopy.<sup>30</sup> These time evolving processes contribute to the observed response at time longer than  $\tau_0$  or  $\tau_\beta$  and are responsible for the broad dispersion customarily identified as the JG relaxation by most workers. After sufficient long times,  $t \gg \tau_0$  or  $\tau_\beta$ , the probability is high that *all* units attempt the primitive relaxation, and the *fully* cooperative  $\alpha$ -relaxation regime (described before in the first paragraph of this section) is reached. In this terminal regime, the  $\alpha$ -relaxation has the maximum dynamic heterogeneity length scale,  $L_{dh}$ , and the Kohlrausch form for the averaged correlation function at the temperature. Naturally, we expect a larger  $L_{dh}$  is associated with a larger  $n$  because both quantities are proportional to many-molecule dynamics. This correlation is borne out by comparing  $n$  with  $L_{dh}$  for glycerol, *o*-terphenyl, and poly(vinyl acetate) obtained by multidimensional <sup>13</sup>C solid-state exchange NMR experiments.<sup>31</sup>

There is experimental evidence that not only  $\tau_\alpha$  but also  $\tau_\beta$  or  $\tau_0$  is dependent on the specific volume  $V$  (or free volume) and entropy  $S$  (or configurational entropy). The CM predicts such a dependence of  $\tau_\beta$  or  $\tau_0$  based on eqs 3–5 and the fact that  $\tau_\alpha$  strongly depends on  $T$ ,  $P$ ,  $V$ , and  $S$ . Good agreement of  $\tau_0$  values calculated via eq 3 with the experimental  $\tau_\beta$  has been found for many glass-formers in the equilibrium liquid state<sup>19–22,24–26,32–35</sup> as well as in the glassy state.<sup>25</sup> Changes in volume and temperature are related to changes in pressure and entropy because of the thermodynamic relation  $(\partial S/\partial P)_T = (\partial V/\partial T)_P$ .<sup>36</sup> Time being a natural variable, and the fact that  $\tau_\beta$  precedes  $\tau_\alpha$ , implies that the source of the

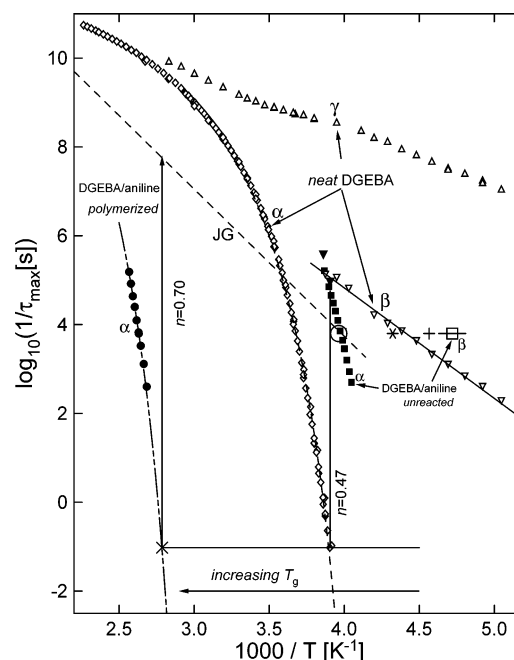


**Figure 1.** Relaxation map for neat EPON828, unreacted mixture of 1 mol of EPON828 with 1 mol of aniline, and partially polymerized and completely polymerized EPON828/aniline mixtures. There are two secondary relaxations in addition to the primary  $\alpha$ -relaxation. Shown are the reciprocals of the  $\alpha$ -relaxation time  $\tau_\alpha$ , the JG  $\beta$ -relaxation time  $\tau_\beta$ , and the non-JG relaxation time  $\tau_\gamma$ . The two solid inverted triangles indicate  $1/\tau_0$  of neat EPON828 calculated at two temperatures just above its  $T_g$ . For the legends of other symbols and lines, and the references from which the data are taken, see text.

dependence of molecular mobility on  $T$ ,  $P$ ,  $V$ , and  $S$  originates from  $\tau_\beta$  or  $\tau_0$ , and the stronger dependence of  $\tau_\alpha$  is obtained by raising them to the superlinear power  $1/(1 - n_\alpha)$  (cf. eqs 2 and 5) as a result of the complex many-molecule dynamics.

In the following sections data for epoxy-containing systems at the various stages of polymerization are discussed. General trends concerning different relaxation processes will be pointed out and confronted with the predictions of the coupling model.

### 3. Neat EPON 828 and Neat Tactix 742 (First Stage)

It is only recently that broadband dielectric relaxation measurements on EPON828<sup>16</sup> and Tactix742 (i.e., T5PMTGE)<sup>17</sup> carried out in the liquid and glassy states have found the existence of two secondary relaxations in addition to the primary relaxation. The faster one ( $\gamma$ -relaxation) has short relaxation time  $\tau_\gamma$  in the nanoseconds range near  $T_g$ , and it does not seem to merge really with the  $\alpha$ -relaxation at a finite temperature. The slower secondary ( $\beta$ -) relaxation has weaker relaxation strength than the  $\gamma$ -relaxation and can only be resolved at temperatures near  $T_g$  and below in the glassy state. When the Arrhenius dependence of its relaxation time  $\tau_\beta$  in the glassy state is extrapolated to temperatures above  $T_g$ , the tendency of it merging with the  $\alpha$ -relaxation time  $\tau_\alpha$  is found. The relaxation map showing the temperature dependence of the most probable relaxation times  $\tau_\alpha$ ,  $\tau_\beta$ , and  $\tau_\gamma$  of neat EPON828 obtained from the data of ref 16 is presented in Figure 1. The dielectric loss data of neat EPON828 at several temperatures above  $T_g$  are presented in Figure 2. The dashed lines are sample fits to the  $\alpha$ -loss peak by the one-sided



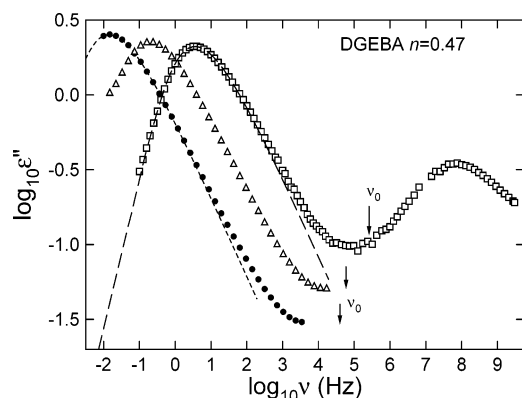


**Figure 2.** Dielectric loss of neat EPON828 at 256, 259, and 263 K, from left to right. The lines are KWW fits to the  $\alpha$ -relaxation peaks with  $n = 0.47$ . Each vertical arrow pointing toward certain data taken at some temperature indicates the location of the independent relaxation frequency,  $\nu_0$ , calculated for that temperature.

Fourier transform of the KWW function with  $n = 0.47$ . It is temperature independent near  $T_g$ , and together with  $\tau_\alpha(T)$ , the corresponding  $\tau_0(T)$  is calculated via eq 3. The calculated values of  $\tau_0(T)$  at  $T = 256$  and  $259$  K are shown in Figure 1 by the two solid inverted triangles. They are in good correspondence with the data of  $\tau_\beta(T)$  near these two temperatures, and thus eq 4 is verified in neat EPON828 as well as in Tactix 742<sup>24</sup> and other molecular and polymeric glass-formers.<sup>19–22,24–26,35</sup> This indicates that slow  $\beta$ -relaxation in EPON828 and Tactix742 is truly of the JG kind according to the criteria proposed recently to classify secondary relaxations.<sup>24</sup> On the other hand, the  $\gamma$ -relaxation appearing at higher frequencies seems to be related to intramolecular motions involving mainly the epoxide end groups and hence is not JG relaxation according to this classification.

The  $\beta$ -relaxation in EPON828 or Tactix742 has weaker dielectric strength compared with the  $\alpha$ - and  $\gamma$ -relaxation, and it can only be resolved at temperatures below  $T_g$ . Verification of the validity of eqs 3–5 is thus limited. However, eqs 3–5 were shown to hold in the case of other glass-formers which have resolved JG  $\beta$ -relaxation in the equilibrium liquid state, detectable either in isobaric spectra<sup>24,25,33–35</sup> at temperatures above  $T_g$  or in isothermal spectra<sup>24,25,32</sup> at pressures less than the glass transition pressure  $P_g$ . On the basis of the generally agreed dependence of  $\tau_\alpha$  on  $T$ ,  $P$ ,  $V$ , and  $S$  and the CM, we expect that  $\tau_\beta$  or  $\tau_0$  should also depend on  $T$ ,  $P$ ,  $V$ , and  $S$ .

#### 4. Unreacted Mixtures of EPON 828 with CHA, Aniline, and PACM (Second Stage)

Neat cyclohexylamine (CHA) and aniline are more mobile than neat EPON828 at the same temperature. Therefore, configurational constraints and intermolecular interaction imposed on EPON828 molecules in their neat form is somewhat mitigated when mixed with CHA or aniline before reaction has begun.

Mitigation of configurational constraints increases configurational entropy and specific volume. This is one cause of the enhancement of molecular mobility, which changes the JG  $\beta$ -relaxation time  $\tau_\beta$  because of its dependence on volume and entropy. Experimental data of the JG  $\beta$ -relaxation of EPON828 in the mixture are rare because of its weak dielectric strength. Nevertheless, there is evidence of it in the EPON 828/aniline

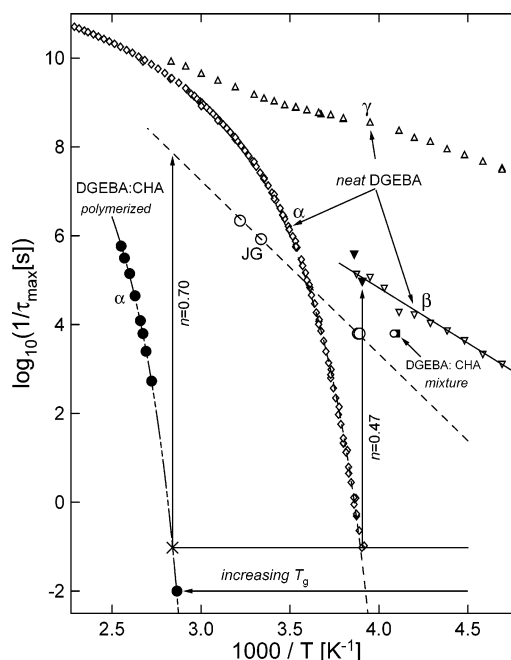


**Figure 3.** Relaxation map for neat EPON828, unreacted mixture of 1 mol of EPON828 with 1 mol of cyclohexylamine (CHA), and partially polymerized and completely polymerized EPON828/CHA mixtures. There are two secondary relaxations in addition to the primary  $\alpha$ -relaxation. Shown are the reciprocals of the  $\alpha$ -relaxation time  $\tau_\alpha$ , the JG  $\beta$ -relaxation time  $\tau_\beta$ , and the non-JG relaxation time  $\tau_\gamma$ . The two solid inverted triangles indicate  $1/\tau_0$  of neat EPON828 calculated at two temperatures just above its  $T_g$ . For the legends of other symbols and lines, and the references from which the data are taken, see text.

mixture from the bump at about 211 K seen in the 1 kHz isochronal dielectric loss data<sup>10</sup> (hollow square in Figure 1). Although the uncertainty of this data point is large, it indicates that  $\tau_\beta$  becomes faster in the mixture than in neat EPON828. Unfortunately, the JG  $\beta$ -relaxation has not been resolved in unreacted mixtures with CHA (Figure 3) and PACM (Figure 4), and we cannot provide additional data supporting a shift of the  $\beta$ -process in unreacted mixtures. On the other hand, the relaxation time  $\tau_\gamma$  of the  $\gamma$ -relaxation of EPON828 or Tactix742 seems to remain relatively unchanged when mixed with the other molecular liquids. This is an indication that the  $\gamma$ -relaxation involves very local motions of the epoxide groups, and hence  $\tau_\gamma$  is insensitive to mixing with other molecular liquids and shows that there are differences between  $\beta$  and  $\gamma$ .

Isothermal as well as isochronal relaxation data of  $\tau_\alpha$  of EPON828 in the mixtures are available<sup>9–13</sup> and shown in Figures 1, 3, and 4 by solid squares. Compared with neat EPON828,  $\tau_\alpha$  of EPON828 in unreacted mixtures with CHA and PACM becomes much shorter as expected. The change of  $\tau_\alpha$  in mixing with PACM is significantly less (Figure 4). This is understandable because PACM is a solid at 293 K, which was molten by heating to 300 K and used as such. In any case the decrease of  $\tau_\alpha$  of EPON828 with mixing is much larger than the decrease of  $\tau_\beta$ . This follows from the CM for mixtures<sup>37–40</sup> because both  $\tau_\beta$  and  $n$  decreases with mixing, and they act in concert to yield a much shorter  $\tau_\alpha$  given by eq 5. Mitigation of intermolecular coupling on mixing should lead to a smaller coupling parameter  $n$  of the EPON828 component in mixtures and reduce the slowing of the  $\alpha$ -relaxation by the many-body dynamics. However, concentration

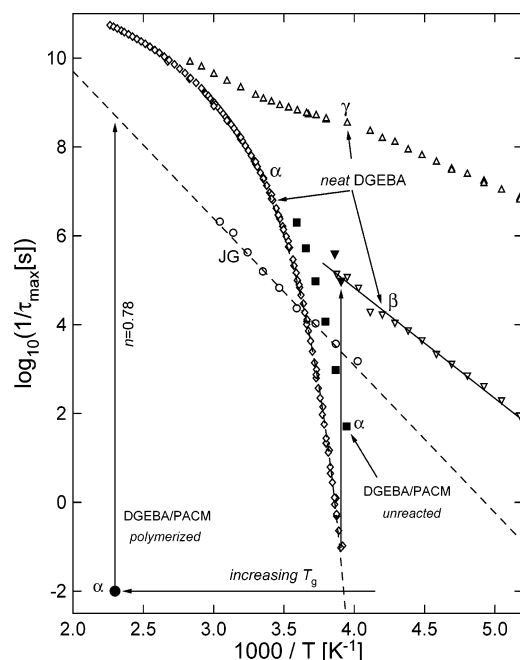


**Figure 4.** Relaxation map for neat EPON828, unreacted mixture of 2 mol of EPON828 with 1 mol of *p*-aminodicyclohexylmethane (PACM), and partially polymerized and completely polymerized EPON828/PACM mixtures. There are two secondary relaxations in addition to the primary  $\alpha$ -relaxation. Shown are the reciprocals of the  $\alpha$ -relaxation time  $\tau_\alpha$ , the JG  $\beta$ -relaxation time  $\tau_\beta$ , and the non-JG relaxation time  $\tau_\gamma$ . The two solid inverted triangles indicate  $1/\tau_0$  of neat EPON828 calculated at two temperatures just above its  $T_g$ . For the legends of other symbols and lines, and the references from which the data are taken, see text.

fluctuations<sup>38–40</sup> are omnipresent in unreacted mixtures and tend to broaden the  $\alpha$ -relaxation of the components. Hence, the reduction of  $n$  of EPON828 in the unreacted mixtures cannot be directly verified by comparing the widths of the dielectric  $\alpha$ -relaxation peaks.

When eq 5 is rewritten as

$$(\log \tau_\alpha - \log \tau_\beta) = n(\log \tau_\alpha - \log t_c) \quad (6)$$

it indicates that for a fixed value of  $\tau_\alpha$ , say 100 s, the separation between  $\tau_\alpha$  and  $\tau_\beta$  decreases as  $n$  becomes smaller. This prediction can be tested if data of  $\tau_\alpha$  and  $\tau_\beta$  become available for the unreacted EPON828 mixtures at the same temperature near  $T_g$ . Previously, the prediction has been verified in mixtures of sorbitol with water, xylitol with water,<sup>39</sup> sorbitol with glycerol,<sup>40</sup> and copolymers of *n*-butyl methacrylate and styrene.<sup>19b</sup>

### 5. Partially Polymerized States (Third Stage)

While mixing EPON828 with aniline, CHA, EDA, HMDA, or PACM has the effect of mitigating the configurational constraint and intermolecular interaction of EPON828 molecules, naturally after reaction starts the covalent bonds formed during the growth of linear chain or network have the opposite effect. The configurational constraint and intermolecular interaction of EPON828 molecules are enhanced monotonically when the polymerization process proceeds, and the complete system becomes more densely packed. This has the effect of slowing down the molecular motion and is illustrated by our new isothermal dielectric data of EPON828/EDA mixture. Figure 5 shows spectra of the

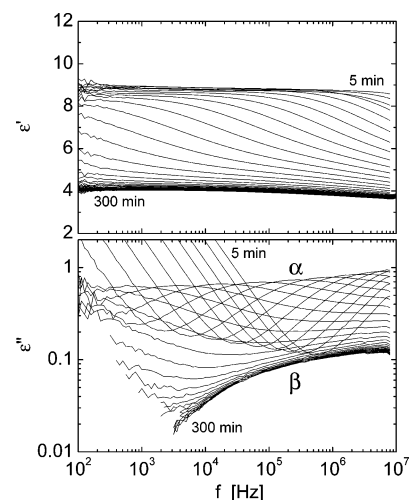


**Figure 5.** Dielectric permittivity  $\epsilon'$  and loss  $\epsilon''$  spectra for a stoichiometric DGEBA/EDA mixture recorded every 5 min during isothermal polymerization at 313 K.

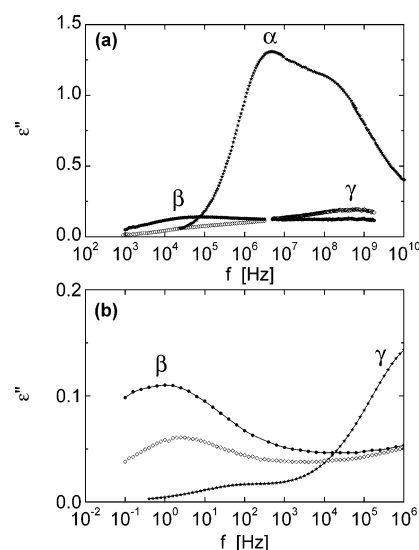


**Figure 6.** Dielectric loss as obtained from isothermal measurements at (a) 297 K and (b) 203 K on unpolymerized EPON828 ( $\star$ ) and on EPON828/EDA mixtures after polymerization for 24 h at  $T_{\text{poly}} = 297$  K ( $\diamond$ ) and at  $T_{\text{poly}} = 343$  K ( $\bullet$ ).

permittivity,  $\epsilon'$ , and loss,  $\epsilon''$ , measured at different times during the polymerization of the molecular liquid at a fixed temperature,  $T_{\text{poly}}$ . During the polymerization process the  $\alpha$ -relaxation peak continuously shifts toward lower frequency. After it has moved out of the low-frequency side of our measurements range, the low-frequency part of a broad secondary relaxation peak emerges in the highly viscous or apparently glassy polymeric state of the EPON828/EDA mixture. To get a better impression of the changes in the  $\alpha$ -,  $\beta$ -, and  $\gamma$ -relaxations during the polymerization process, isothermal  $\epsilon''$  spectra measured at  $T = 297$  and at  $T = 203$  K of the neat EPON828 are compared with that of DGEBA/EDA mixtures polymerized for 24 h at  $T_{\text{poly}} = 297$  K and  $T_{\text{poly}} = 343$  K in Figure 6. At  $T = 297$  K (Figure 6a), the dielectric loss of the neat EPON828<sup>16</sup> shows the peak of the  $\alpha$ -relaxation and a shoulder on its high-frequency side belonging to the  $\gamma$ -process. After polymerized for 24 h at  $T_{\text{poly}} = 297$  K ( $\diamond$ ) the  $\alpha$ -relaxation is outside the experimental window. The  $\gamma$ -relaxation remains at nearly the same frequency, but its intensity is reduced. More covalent bonds are formed

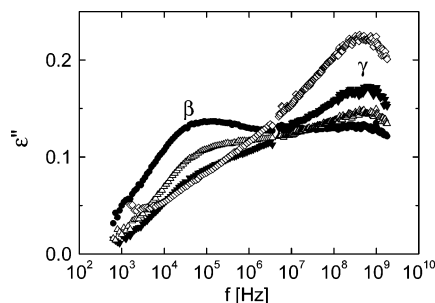


**Figure 7.** Dielectric loss spectrum measured at  $T = 297 \pm 1$  K of EPON828/EDA after it has been polymerized for 5 h at several temperatures:  $T_{\text{poly}} = 298$  ( $\diamond$ ), 313 ( $\blacktriangledown$ ), 328 ( $\triangle$ ), and 343 K ( $\bullet$ ).

in the EPON828/EDA mixture polymerized for the same duration of 24 h but at a higher temperature of  $T_{\text{poly}} = 343$  K. Its dielectric loss data in Figure 6a ( $\bullet$ ) show further decrease of the  $\gamma$ -relaxation intensity and the emergence of a resolved  $\beta$ -relaxation. Dielectric measurement on the same three materials were also made at a lower temperature of 203 K (Figure 6b). These isotherms show that a weak  $\beta$ -relaxation is already present in neat EPON828, and it grows in intensity and shifts to lower frequencies during polymerization. Figure 7 shows the secondary relaxations  $\beta$  and  $\gamma$  in  $\epsilon''$  isotherms measured at  $T = 297$  K after polymerizing EPON828/EDA mixtures for 5 h at  $T_{\text{poly}} = 368, 313, 328$ , and 343 K. The spectra show that the intensity of the  $\gamma$ -relaxation peak decreases and that of the  $\beta$ -relaxation peak increases when polymerization of the EPON828/EDA mixtures is performed at higher temperatures, resulting in more covalent bonds formed. Ultimately, the intensity of the  $\gamma$ -relaxation becomes so small that the peak in  $\epsilon''$  cannot be discerned. The trends in these isothermal data are typical for the evolution of the various relaxation peaks as polymerization proceeds. The trends are basically independent of the molecular structure of the EPON828-containing system, as shown before by isochronal dielectric measurements.<sup>2,9–11</sup> Our isothermal data offer a complementary way to visualize the changes of the relaxation processes with the increase of the number of covalent bonds. Note that the increase of the  $\beta$  relaxation strength  $\Delta\epsilon_{\beta}$  with number of bonds formed during the polymerization process is opposite to the usually observed decrease in  $\Delta\epsilon_{\beta}$  with time during physical aging. This indicates that the changes in the relaxation behavior are primarily due to changes in the molecular structure.

We have also performed dielectric measurements in a wide temperature range below  $T_g$  on EPON828/EDA mixtures which have been polymerized for 5 h at three different temperatures  $T_{\text{poly}}$ . A representative example is shown in Figure 8. The loss peak frequencies,  $f_{m\beta}$  and  $f_{m\gamma}$ , for the  $\beta$ - and  $\gamma$ -relaxations have been taken out. The results expressed as the angular frequencies  $2\pi f_{m\beta} \equiv (1/\tau_{\beta})$  and  $2\pi f_{m\gamma} \equiv (1/\tau_{\gamma})$  are plotted against reciprocal temperature in Figure 9. The temperature dependences are Arrhenius-like with an average activation energy  $E_{\beta}$  and  $E_{\gamma}$  of  $60 \pm 6$  kJ/mol and  $28 \pm 3$  kJ/mol for the  $\beta$ - and  $\gamma$ -relaxations, respectively. For comparison, we have included data for the  $\beta$ - and  $\gamma$ -processes in pure DGEBA taken from ref 16 ( $E_{\beta} = 47.6$  kJ/mol;  $E_{\gamma} = 28$  kJ/mol).

The increase of configurational constraint decreases the configurational contributions to the volume, enthalpy, and entropy. Hence, from the proposed depen-

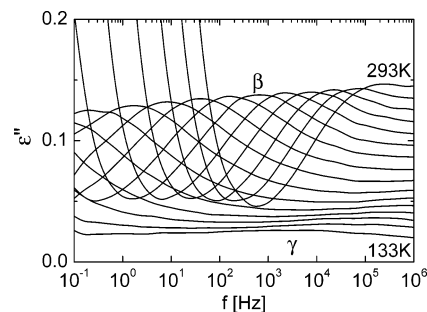


**Figure 8.** Dielectric loss  $\epsilon''$  vs logarithm of frequency measured at different temperatures between 293 and 133 K (temperature step 10 K) in the glassy state of a EPON828/EDA sample polymerized at 313 K for 5 h.

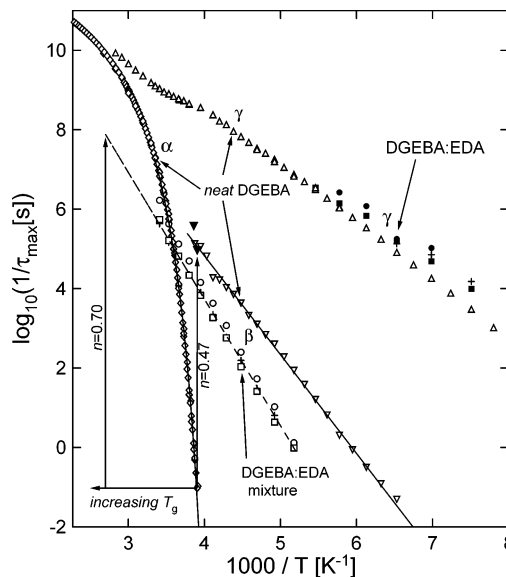


**Figure 9.** Arrhenius plot of the  $\beta$ - and  $\gamma$ -relaxation angular frequencies of EPON828/EDA after it has been polymerized for 5 h at three different temperatures (circles, 313 K; squares, 328 K; +, 343 K). Shown also are the reciprocals of the  $\alpha$ -relaxation time  $\tau_{\alpha}$ , the JG  $\beta$ -relaxation time  $\tau_{\beta}$ , and the non-JG relaxation time  $\tau_{\gamma}$  of neat EPON828 from ref 16. The two solid inverted triangles indicate  $1/\tau_0$  of neat EPON828 calculated at two temperatures just above its  $T_g$ .

dence of  $\tau_{\beta}$  on volume and entropy in the CM (see section 2),  $\tau_{\beta}$  should become longer with the increase of  $N(t)$ . This trend can be clearly seen from the isothermal dielectric data for EPON828/EDA in Figures 6b, 7, and 9, but it was also observed in previous isochronal measurements on similar systems. Dielectric measurements at 1 kHz show that the temperature  $T_{\beta}$  at which  $\tau_{\beta}$  corresponds to this frequency moves appreciably to higher temperatures. For the EPON828/aniline mixture, this trend is shown in Figure 1, where the cross (+), the star (\*), and the large hollow circle ( $\circ$ ) indicate the temperatures  $T_{\beta}$  of the slightly polymerized ( $N = 0.339 \times 10^{23}$ ), half-polymerized ( $N = N(\infty)/2$ ), and the completely polymerized ( $N = N(\infty) \approx 6 \times 10^{23}$ ) states, respectively.<sup>10</sup> For the EPON828/CHA mixture<sup>12</sup> (Figure 3), the smaller ( $\circ$ ) and the larger ( $\circ$ ) hollow circles indicate the  $T_{\beta}$  values of the half polymerized ( $N = N(\infty)/2$ ), and the completely polymerized ( $N = N(\infty) \approx 6 \times 10^{23}$ ) states, respectively. The monotonic increase of  $T_{\beta}$  with increasing number of covalent bonds formed  $N(t)$  is obviously a general feature of such systems. This can be concluded from isochronal  $\epsilon''$  data<sup>10</sup> for the mixtures described above and from results for more than 10



mixtures of EPON828 with other molecular liquids which form linear polymers or networks.<sup>9</sup> More data of  $T_\beta$  at different  $N(t)$  could be included in Figures 1 and 3 to demonstrate the increase of  $\tau_\beta$  during the reaction. Data points for the  $\beta$ -relaxation of a completely polymerized EPON828/PACM<sup>13</sup> mixture (o, Figure 4) support this view.

The isothermally measured relaxation times  $\tau_\beta$  for completely polymerized EPON828/CHA<sup>12</sup> (○, Figure 3) and EPON828/PACM<sup>13</sup> (o, Figure 4) mixtures indicate an Arrhenius-like temperature dependence in the glassy state. The activation energies are  $E_\beta$  of 72 and 63.4 kJ/mol for EPON828/CHA and EPON828/PACM, respectively. These values of  $E_\beta$  for the polymerized structures are higher than 47.6 kJ/mol of neat EPON828, in agreement with the findings for the EPON828/EDA system. Note that the changes in the relaxation times  $\tau_\alpha$  and  $\tau_\beta$  during polymerization result in a shift of the  $\alpha\beta$  crossover region, where  $\alpha$ - and  $\beta$ -relaxation times become comparable.<sup>16</sup> An extrapolation indicates an increase in the crossover temperature  $T_c$  (sometimes called the Donth temperature) and a decrease in the crossover times  $\tau_c$  during reaction.

The  $\gamma$ -relaxation of neat EPON828 arises from the motion of localized dipoles of the epoxide end groups. From broadband dielectric data<sup>16</sup> the temperature  $T_\gamma$  at which its relaxation time  $\tau_\gamma$  correspond to the frequency of 1 kHz is 138 K. It is present in the unreacted mixture as well as after reaction has started, with no noticeable change in  $T_\gamma$ .<sup>9–12</sup> Reaction in the mixture consumes the epoxide groups and naturally the relaxation strength of the  $\gamma$ -relaxation process in the mixtures gradually decreased and the process approached extinction as the number of covalent bonds approached its limiting value. This behavior of  $\tau_\gamma$  is unlike the JG  $\beta$ -relaxation time  $\tau_\beta$ , which is shifted toward shorter times after mixing but before reaction starts and in the opposite direction increasingly with covalent bonds formed by reactions. These differences between  $\tau_\beta$  and  $\tau_\gamma$  in their response to mixing, polymerizing, and networking might be an addition to various properties listed in ref 24 to distinguish JG relaxations from non-JG secondary relaxations.

Isothermal dielectric data of  $\tau_\alpha$  are available for completely polymerized EPON828/aniline and EPON828/CHA mixtures. They are shown by the solid circles in Figures 1 and 3. For EPON828/PACM mixtures, the glass-softening temperature of the fully cross-linked state was reported<sup>13</sup> to be higher than 435 K. This is the only information given on the  $\alpha$ -relaxation. The solid circle in Figure 4 at (1000/435 K<sup>-1</sup>,  $\log(1/\tau_\alpha) = -2$ ) marks a crude estimate of the location of the  $\alpha$ -relaxation at  $T_g$ . By inspection of all three relaxation maps, on increasing the number of covalent bonds  $N(t)$ , it is clear that the shift of  $\tau_\alpha$  to longer times (isothermally) or to higher temperatures (isochronically) is accompanied by a shift of  $\tau_\beta$ , albeit the former is much larger than the latter. As mentioned before, the observed shifts of  $\tau_\beta$  with increase of  $N$  support the CM view that dependence of molecular mobility on volume and entropy enter into  $\tau_\beta$  first. The larger shifts of  $\tau_\alpha$  is consistent with eq 5 of the CM, which magnifies any change of  $\tau_\beta$  by raising it to the superlinear power of  $1/(1 - n)$ . Furthermore, the shift of  $\tau_\alpha$  relative to that of  $\tau_\beta$  is larger if  $N$  is larger. This trend is again consistent with eq 5 because the coupling parameter  $n$  increases with  $N$  indicated by decreasing stretch expo-

nents  $\beta \equiv (1 - n)$ . Isothermal dielectric data of the  $\alpha$ -relaxation in partially polymerized EPON 828/CHA mixtures ( $N = 4.04 \times 10^{23}$ ) at 314.2 K indicate  $\tau_\alpha \approx 10^{-4}$  s. The dispersion of the  $\alpha$  loss peak is very broad, having a full width at half-maximum of 3 decades, and a reported stretch exponent  $\beta = 0.39$  from a fit by the KWW function (eq 2).<sup>12</sup> The loss peak of partially (45%) polymerized and cross-linked EPON828/PACM mixture at 308.2 K with  $\tau_\alpha \approx 10^{-4.3}$  s has a full width at half-maximum of 3.5 decades and a reported  $\beta = 0.32$ .<sup>13</sup> One can expect that the fully polymerized EPON828/CHA linear chains or the 100% cross-linked EPON828/PACM network with more configurational restrictions would have an even broader dispersion, particularly at longer  $\tau_\alpha \approx 10^2$  s. This is to be compared with the full width at half-maximum of about 2 decades of neat EPON828. Works by others<sup>14,15</sup> on EPON828/EDA and EPON828/*n*-butylamine mixtures have acquired isothermal dielectric data on the dispersion of the  $\alpha$ -relaxation and showed that it broadens monotonically with increasing number of covalent bonds. For 80% conversion of the EPON828/EDA mixture and for 73% conversion of the EPON828/*n*-butylamine, the broad dispersions of the  $\alpha$ -relaxation were described by the Havriliak–Negami parameters, which correspond approximately to KWW stretch exponents  $\beta$  of 0.36 and 0.30, respectively. Thus, all experimental data of  $\alpha$ -relaxation in partially polymerized systems support consistently an increase of the coupling parameter  $n$  with increasing number of covalent bonds  $N$ . Additional support for the same comes from the changes of the JG  $\beta$ -relaxation with  $N(t)$ . First argument is the observed monotonic increase of the height, or strength, of the  $\beta$ -relaxation peak relative to that of the  $\alpha$ -relaxation. As suggested by empirical facts,<sup>20,27</sup> this trend is accompanied by an increase of the coupling parameter  $n$ . Second argument is the increase of the difference, ( $\log \tau_\alpha - \log \tau_\beta$ ), at constant  $\log \tau_\alpha$ . According to eq 6, this indicates an increase of  $n$  with  $N(t)$ .

To determine  $n$  values from  $\tau_\alpha$  and  $\tau_\beta$  using eq 6 both times have to be available at the same temperature. This information is hard to get for polymerizing mixtures and only available for completely polymerized or cross-linked systems. This stage is discussed in the following section.

## 6. Completely Polymerized and Cross-Linked State (Final Stage)

In all the experiments discussed in this work, the only stage other than the neat diepoxides that one can characterize both the  $\alpha$ -relaxation and the JG  $\beta$ -relaxation is when polymerization or cross-linking of the mixture has been carried out to completion. Even in this case, some extrapolations of the data of both  $\tau_\alpha$  and  $\tau_\beta$  have to be performed before eq 6 can be used to calculate  $n$  values and to compare them with  $n$  values estimated based on the stretch exponent  $\beta$ .

For the completely polymerized EPON828/CHA and EPON828/aniline mixtures, the data of  $\tau_\alpha$  over limited range of temperature are interpolated or extrapolated to lower temperatures by a fit to the Vogel–Fulcher–Tammann–Hesse equation (line passing over solid circles in Figures 1 and 3). For the fully cross-linked EPON/PACM, only an estimate of  $\tau_\alpha$  at one temperature (the lone solid circle in Figure 4) can be made from the information<sup>13</sup> that the glass-softening temperature is higher than 435 K. The JG  $\beta$ -relaxation times  $\tau_\beta$  of the

fully reacted EPON828/CHA (○, Figure 3) and EPON828/PACM (○, Figure 4) were given over a range of temperatures, and they show an Arrhenius temperature dependence in the glassy state (dashed lines). There is only one data point of  $\tau_\beta$  of the fully polymerized EPON828/aniline from isochronal measurement at 1 kHz (large hollow circle in Figure 1). Assuming that its activation energy is the same as  $\tau_\beta$  of the fully cross-linked EPON828/PACM, the dashed line through the hollow circle represents  $\tau_\beta$  of the fully reacted EPON828/aniline.

Since all JG relaxation times  $\tau_\beta$  obey the Arrhenius law at temperatures below  $T_g$ , these fits when extrapolated to higher temperatures should give good estimates of  $\tau_\beta$  at some temperature near  $T_g$  where  $\tau_\alpha$  is known either directly or by extrapolation. For the completely polymerized EPON828/CHA and EPON828/aniline mixtures, we choose the temperature at which  $\tau_\alpha$  is 10 s like previously done for neat EPON828 and indicated by the horizontal line in Figures 1 and 3. At this temperature  $\tau_\beta = 10^{-7.8}$  and  $10^{-7.7}$  s for the completely polymerized EPON828/CHA and EPON828/aniline, respectively. With both  $\tau_\alpha$  and  $\tau_\beta$  known, the coupling parameter  $n$  of the completely polymerized EPON828/CHA and EPON828/aniline when  $\tau_\alpha = 10$  s is calculated by eq 6. The result is

$$n = 0.69 \quad (7)$$

for both systems. Such a large value of  $n$  is consistent with the very broad dispersion of the  $\alpha$ -relaxation corresponding to a KWW stretched exponent  $\beta \equiv (1 - n) = 0.39$  found in partially polymerized states at shorter  $\tau_\alpha$  discussed in the previous section. Such a low value of  $\beta$ , or equivalently a broader distribution of relaxation times, found generally in the EPON828-containing polymers has been rationalized in ref 12 as a reflection of the large repeat units in the structure of this kind of polymers. The  $\alpha$ -relaxation time of the fully polymerized EPON828/EDA mixture has not been determined, and its  $n$  value cannot be calculated by this procedure. If we assume that it has the value of 0.70, similar to that found for the other two fully polymerized mixtures, one gets from eq 6 a  $T_\alpha$  value for  $\tau_\alpha = 10$  s, which is given by the location of the long vertical arrow in Figure 9.

For the completely cross-linked EPON828/PACM at 435 K where  $\tau_\alpha = 100$  s and  $\tau_\beta = 10^{-8.7}$  s, obtained by extrapolating the Arrhenius dependence given in ref 13, the coupling parameter  $n$  calculated by eq 6 has even a larger value

$$n = 0.78 \quad (8)$$

Again, such large value is consistent with a very broad  $\alpha$ -relaxation loss peak expected for the 100% reacted state based on the data of 45% reacted state. The loss peak of the 45% reacted state already has a KWW stretch exponent  $\beta = 0.32$  at a much shorter  $\tau_\alpha \approx 10^{-4.3}$  s.<sup>13</sup> It is also consistent with the fact that the completely reacted EPON828/PACM has a much higher  $T_g$  than the fully polymerized EPON828/CHA and EPON828/aniline, indicating more severe configurational restrictions. Note that fully reacted EPON828/PACM mixtures which show very broad  $\alpha$  peaks and large coupling parameters  $n$  are network forming systems while EPON828/CHA and EPON828/aniline mixtures with smaller  $n$  values form linear chains. Although the

difference in  $n$  may appear small, the effect on slowing the  $\alpha$ -relaxation is much more spectacular in the networks than linear chains because what counts in eqs 3 and 5 is the exponent,  $1/(1 - n)$ . In general, EPON828-based networks seem to have slightly larger  $n$  values compared to systems forming linear chains.

## 7. Similar Results from a Triepoxide

Dielectric measurements have been made to follow the evolution of the primary and secondary relaxations starting from the unreacted mixtures of the triepoxide, Tactix742 (i.e., triphenylolmethane triglicidyl ether (TPMTGE)) with aniline, 3-chloraniline, and 4-chloroaniline.<sup>10</sup> Neat Tactix742 has a faster  $\gamma$ -relaxation<sup>17</sup> which comes from the local motion of the epoxide groups and a slower  $\beta$ -relaxation which has been shown to be a JG secondary relaxation.<sup>24</sup> One evidence for the latter is the good agreement of its relaxation time  $\tau_\beta$  with the independent relaxation time  $\tau_0$  calculated at temperatures near  $T_g$ .<sup>24</sup> The changes of  $\tau_\beta$  in the passage from the unreacted mixture to the completely polymerized state are similar as that described in previous sections for EPON828 mixtures. The  $\gamma$ -relaxation relaxation time changed little, but its strength in the Tactix742 mixtures gradually decreased and the process approached extinction as the number of covalent bonds approached its limiting value. Concurrently, the JG  $\beta$ -relaxation in the glassy state grew in strength, and its relaxation time  $\tau_\beta$  was shifted to longer times as more covalent bonds were formed and the glass transition temperature is increased. The reported experimental results of the Tactix742 mixtures do not have sufficient detail to allow quantitative analysis. Nevertheless, the effects observed transcend the details of the chemical and physical structures of the starting molecular liquid and the final product.

## 8. Discussion and Conclusion

For the purpose of distinguishing between the observed secondary relaxations and the  $\beta$ -process of mode coupling theory these days, it has become a common practice to call all of them Johari–Goldstein (JG) relaxation. Recently, an effort has been made to classify secondary relaxation by differentiating their properties and gives a more restricted definition of JG relaxation.<sup>24</sup> In so doing, there should be only one true JG secondary relaxation in any glass-former, and it bears fundamental relations to the  $\alpha$ -relaxation and is instrumental for glass transition. Conceptually this is clear in totally rigid glass-formers where there is only one secondary relaxation, and its motion triggers the many-molecule cooperative  $\alpha$ -relaxation. Any other secondary relaxation present, usually at shorter times, likely involves local motion of a smaller part of the molecule and are decoupled from the  $\alpha$ -relaxation. The neat diepoxide EPON828 and triepoxide Tactix742 are examples of molecular glass-formers that have two secondary relaxations, and they offer excellent opportunity of showing the difference in their properties as well as supporting the existence of relations between the true JG relaxation and the  $\alpha$ -relaxation. In this work we have tapped the tremendous amount of work on the evolution of the primary and the two secondary relaxations with reaction time, conversion, or the number of covalent bonds formed. The results are qualitatively the same, independent of the structure of the molecular liquids. Collectively they show that the  $\gamma$ -relaxation time  $\tau_\gamma$  is



basically insensitive to mixing before reaction starts and polymerization thereafter. In contrast, the JG relaxation time  $\tau_\beta$  becomes shorter in the unreacted mixture of the diepoxide or the triepoxide with a more mobile molecular liquid, and after reaction has started it reverses direction to increase monotonically during the polymerization process. These changes of  $\tau_\beta$  correlate with that of  $\tau_\alpha$ , the  $\alpha$ -relaxation time, although the changes of  $\tau_\alpha$  are much larger. The increase (decrease) of the configurational restriction of molecular motion and decrease (increase) of the specific volume with the number of covalent bonds formed (mixing) imply the decrease (increase) of configurational entropy or free volume. Hence, the changes of  $\tau_\beta$  observed can be considered as evidence that the JG relaxation time already depends on (configurational) entropy or free volume before the  $\alpha$ -relaxation transpires. This is an important experimental finding on JG relaxation that supports the deduction from the coupling model (CM).

Accompanying the increase of  $\tau_\alpha$  with formation of polymer networks or linear chain polymers from small epoxy resin molecules is the increase of the width of the dispersion of the  $\alpha$ -relaxation time. When interpreted in terms of the CM, this is equivalent to the increase of the coupling parameter  $n$  or the slowing of the cooperative many-molecule  $\alpha$ -relaxation. Two results of the CM given by eqs 4–6 indicate that (i)  $\tau_\beta$  is approximately the same as the independent relaxation time  $\tau_0$  and (ii) the separation of the two relaxation times given by  $(\log \tau_\alpha - \log \tau_\beta)$  increases with coupling parameter  $n$  or  $N$ , the number of covalent bonds formed by reaction. The first result is verified quantitatively in the neat diepoxide and triepoxide and qualitatively consistent in other stages of the experiment. The second result is also in qualitative agreement with the changes in relation between the two relaxation times at all stages of the experiment. For the completely polymerized or cross-linked product, the large values of the coupling parameter  $n$  deduced from the experimentally determined separation distances  $(\log \tau_\alpha - \log \tau_\beta)$  by using eq 6 are consistent with the small KWW exponents or large widths of the  $\alpha$ -relaxation found already in the states that have not been fully polymerized or cross-linked. A similar relation between secondary relaxation time and the  $\alpha$ -relaxation time but different in quantitative details was given by Cavaille et al.<sup>41</sup> in their model of relaxation in glass-formers.

**Acknowledgment.** This work was supported by the Office of Naval Research. M.B. thanks G. P. Johari for financial support during his visit at the McMaster University where some of the dielectric data for the EPON828/EDA system have been measured.

## References and Notes

- (1) *Proceedings of the 47th Annual Technical Conference of Society of Plastics Engineers (SPE ANTEC '89)*, New York, 1989.
- (2) (a) Johari, G. P. Dynamics of irreversibly forming macromolecules. In *Disorder Effects in Relaxational Processes*; Richert, R., Blumen, A., Eds.; Springer-Verlag: Berlin, 1994; p 627. (b) Mangion, M. B. M.; Johari, G. P. *J. Polym. Sci., Part B: Polym. Phys.* **1990**, *28*, 71; **1990**, *28*, 1621; **1991**, *29*, 437.
- (3) (a) Fitz, B.; Andjelic, S.; Mijovic, J. *Macromolecules* **1997**, *30*, 5227. (b) Andjelic, S.; Fitz, B.; Mijovic, J. *Macromolecules* **1997**, *30*, 5239.
- (4) (a) Corezzi, S.; Fioretto, D.; Rolla, P. *Nature (London)* **2003**, *420*, 653. (b) Corezzi, S.; Fioretto, D.; Puglia, D.; Kenny, J. M. *Macromolecules* **2003**, *36*, 5271.
- (5) (a) Lee, A.; McKenna, G. B. *Polymer* **1990**, *31*, 423. (b) Lee, A.; McKenna, G. B. *Polymer* **1988**, *29*, 1812.
- (6) Plazek, D. J.; Chay, I.-C. *J. Polym. Sci., Part B: Polym. Phys. Ed.* **1991**, *29*, 17.
- (7) (a) Alig, I.; Johari, G. P. *J. Polym. Sci., Part B: Polym. Phys.* **1993**, *31*, 299. (b) Alig, I.; Lellinger, D.; Johari, G. P. *J. Polym. Sci., Part B: Polym. Phys. Ed.* **1992**, *30*, 791. (c) Parthun, M. G.; Johari, G. P. *J. Chem. Phys.* **1995**, *102*, 6301.
- (8) (a) Monserrat, S.; Gomez-Ribelles, J. L.; Meseguer, J. M. *Polymer* **1998**, *39*, 3801. (b) Hutchinson, J. M.; McCarthy, D.; Monserrat, S.; Cortes, P. *J. Polym. Sci., Part B: Polym. Phys. Ed.* **1996**, *34*, 229. (c) Monserrat, S.; Roman, F.; Colomer, P. *Polymer* **2003**, *44*, 101.
- (9) (a) Parthun, M. G.; Johari, G. P. *Macromolecules* **1992**, *29*, 3254. (b) Parthun, M. G.; Johari, G. P. *J. Chem. Phys.* **1995**, *103*, 7611. (c) Parthun, M. G.; Johari, G. P. *J. Chem. Phys.* **1995**, *103*, 440.
- (10) Wasylyshyn, D. A.; Johari, G. P. *J. Chem. Phys.* **1996**, *104*, 5683.
- (11) (a) Wasylyshyn, D. A.; Parthun, M. G.; Johari, G. P. *J. Mol. Liq.* **1996**, *69*, 283. (b) Wasylyshyn, D. A.; Johari, G. P. *J. Polym. Sci., Part B: Polym. Phys.* **1997**, *35*, 437.
- (12) (a) Tombari, E.; Ferrari, C.; Salvetti, G.; Johari, G. P. *J. Phys.: Condens. Matter* **1997**, *9*, 7017. (b) Ferrari, C.; Tombari, E.; Salvetti, G.; Johari, G. P. *J. Chem. Phys.* **1999**, *110*, 10599.
- (13) (a) Tombari, E.; Ferrari, C.; Salvetti, G.; Johari, G. P. *J. Phys. Chem. Phys.* **1999**, *1*, 1965. (b) Tombari, E.; Salvetti, G.; Johari, G. P. *J. Chem. Phys.* **2000**, *113*, 6957.
- (14) Lairez, D.; Emery, J. R.; Durand, D.; Pethrick, R. A. *Macromolecules* **1992**, *25*, 7208.
- (15) (a) Casalini, R.; Livi, A.; Rolla, P. A.; Levita, G.; Fioretto, D. *Phys. Rev. B* **1996**, *53*, 564. (b) Levita, G.; Livi, A.; Rolla, P. A.; Culicchi, C. *J. Polym. Sci., Part B: Polym. Phys.* **1996**, *34*, 2731. (c) Gallone, G.; Capaccioli, S.; Levita, G.; Rolla, P. A.; Corezzi, S. *Polym. Int.* **2001**, *50*, 545.
- (16) Corezzi, S.; Beiner, M.; Huth, H.; Schröter, K.; Capaccioli, S.; Casalini, R.; Fioretto, D.; Donth, E. *J. Chem. Phys.* **2002**, *117*, 2435.
- (17) Pisignano, D.; Capaccioli, S.; Casalini, R.; Lucchesi, M.; Rolla, P. A.; Justl, A.; Rössler, E. *J. Phys.: Condens. Matter* **2001**, *13*, 4405.
- (18) (a) Ngai, K. L. *Comments Solid State Phys.* **1979**, *9*, 141. (b) Ngai, K. L.; Tsang, K. Y. *Phys. Rev. E* **1999**, *60*, 4511. (c) Ngai, K. L.; Rendell, R. W. In *Supercooled Liquids, Advances and Novel Applications*; Fourkas, J. T. D., Kivelson, U., Mohanty, K., Nelson, Eds.; ACS Symposium Series Vol. 676; American Chemical Society: Washington, DC, 1997; Chapter 4, p 45.
- (19) (a) Ngai, K. L. *J. Chem. Phys.* **1998**, *109*, 6982. (b) Ngai, K. L. *Macromolecules* **1999**, *32*, 7140. (c) Ngai, K. L. *IEEE Trans. Dielectr. Electr. Insul.* **2001**, *8*, 329.
- (20) Ngai, K. L. *J. Phys.: Condens. Matter* **2003**, *15*, S1107.
- (21) Ngai, K. L. *AIP Conf. Proc.* **2004**, *708*, 515.
- (22) Ngai, K. L.; Beiner, M. *Macromolecules* **2004**, *37*, 8123.
- (23) (a) Johari, G. P.; Goldstein, M. *J. Chem. Phys.* **1970**, *53*, 2372. (b) Johari, G. P. *J. Chem. Phys.* **1973**, *58*, 1766. (c) Johari, G. P. *Ann. N. Y. Acad. Sci.* **1976**, *279*, 117. (d) Johari, G. P. *J. Non-Cryst. Solids* **2002**, *307–310*, 317.
- (24) Ngai, K. L.; Paluch, M. *J. Chem. Phys.* **2004**, *120*, 857.
- (25) Prevosto, D.; Capaccioli, S.; Lucchesi, M.; Rolla, P. A.; Ngai, K. L. *J. Chem. Phys.* **2004**, *120*, 4808.
- (26) Ngai, K. L.; Capaccioli, S. *Phys. Rev. E* **2004**, *69*, 031501.
- (27) Ngai, K. L.; J. Habasaki, León, C.; Rivera, A. *Z. Phys. Chem.* **2005**, *219*, 47.
- (28) Sillescu, H.; Böhmer, R.; Diezemann, G.; Hinze, G. *J. Non-Cryst. Solids* **2002**, *307–310*, 16.
- (29) Vogel, M.; Tschirwitz, C.; Schneider, G.; Koplin, C.; Medick, P. *J. Non-Cryst. Solids* **2002**, *307–310*, 326.
- (30) Weeks, E. R.; Crocker, J. C.; Levitt, A.; Schofield, A.; Weitz, D. A. *Science* **2000**, *287*, 627.
- (31) Reinsberg, S. A.; Heuer, A.; Doliwa, B.; Zimmermann, H.; Spiess, H. W. *J. Non-Cryst. Solids* **2002**, *307–310*, 208.
- (32) Casalini, R.; Roland, C. M. *Phys. Rev. Lett.* **2003**, *91*, 015702; *Phys. Rev. B* **2004**, *69*, 094202.
- (33) Ngai, K. L.; Lunkenheimer, P.; León, C.; Schneider, C. U.; Brand, R.; Loidl, A. A. *J. Chem. Phys.* **2001**, *115*, 1405.
- (34) Paluch, M.; Roland, C. M.; Pawlus, S.; Ziolo, J.; Ngai, K. L. *Phys. Rev. Lett.* **2003**, *91*, 115701.

- (35) Sanz, A.; Nogales, A.; Ezquerra, T. A.; Lotti, N.; Finelli, L. *Phys. Rev. E* **2004**, *70*, 021502.
- (36) Lewis, G. N.; Randall, M. *Thermodynamics*, 2nd ed.; McGraw-Hill: New York, 1961.
- (37) Santangelo, P. G.; Roland, C. M.; Ngai, K. L.; Rizos, A. K.; Katerinopoulos, H. *J. Non-Cryst. Solids* **1994**, *172–174*, 1084.
- (38) Ngai, K. L.; Roland, C. M. *Rubber Chem. Technol., Rubber Rev.* **2004**, *77*, 579.
- (39) Psurek, T.; Maslanka, S.; Paluch, M.; Nozaki, R.; Ngai, K. L. *Phys. Rev. E* **2004**, *70*, 011503.
- (40) Ngai, K. L.; Capaccioli, S. *J. Phys. Chem. B* **2004**, *108*, 11118.
- (41) Cavaille, J. Y.; Perez, J.; Johari, G. P. *Phys. Rev. B* **1989**, *39*, 2411.

MA050384J